

See discussions, stats, and author profiles for this publication at: <https://www.researchgate.net/publication/263875785>

Analysis of generalized stress intensity factors of V-shaped notch problems by FEM

Article in *International Journal of Computational Methods* · May 2013

DOI: 10.1142/S0219876213500680

CITATIONS

8

READS

239

4 authors, including:



Xuecheng Ping

Tianjin University of Science and Technology

69 PUBLICATIONS 506 CITATIONS

[SEE PROFILE](#)



Meng-Cheng Chen

East China Jiaotong University

19 PUBLICATIONS 235 CITATIONS

[SEE PROFILE](#)



Nao-Aki Noda

Kyushu Institute of Technology

695 PUBLICATIONS 3,769 CITATIONS

[SEE PROFILE](#)

ANALYSIS OF GENERALIZED STRESS INTENSITY FACTORS OF V-SHAPED NOTCH PROBLEMS BY FEM

XUE-CHENG PING^{*,§}, MENG-CHENG CHEN^{†,¶,††},
NAO-AKI NODA^{‡,||} and YI-HUA XIAO^{*,**}

^{*}*School of Mechatronics Engineering, East China Jiaotong University
Nanchang, Jiangxi 330013, P. R. China*

[†]*School of Civil Engineering, East China Jiaotong University
Nanchang, Jiangxi 330013, P. R. China*

[‡]*Department of Mechanical Engineering, Kyushu Institute of Technology
1-1, Sensui-cho, Tobata, Kitakyushu 804-8550, Japan*

[§]*xuecheng-ping@yahoo.com.cn*

[¶]*mengcheng_chen@yahoo.com.cn*

^{||}*noda@mech.kyutech.ac.jp*

^{**}*xyhtome@yahoo.com.cn*

Received 20 February 2011

Accepted 31 December 2011

Published 24 April 2013

This paper deals with a finite element method (FEM) based on a V-shaped notch corner tip stresses to solve generalized stress intensity factors (GSIFs) in 2D elastic bodies. The method does not need extremely refined meshes and special elements accounting for the analytical form of singularities around the V-shaped notch corner tip. The generalized stress intensity factors of the V-shaped notch problems are evaluated from the ratios of FEM stress values at the notch corner tip for a given problem and a reference one. Several numerical examples show that present method is effective and applicable to dealing with the V-shaped notch problems.

Keywords: Elasticity; V-shaped notch; stress field; GSIF; FEM.

1. Introduction

Strong stress concentrations are usually occurred around notch tips, so the presence of notches may result in crack initiation and finally lowering the loading capacity of structural members. The knowledge of fracture behavior or mechanism of such a structure member is very important for many engineering applications. The fracture is related to stress singularities and stress fields around the V-shaped notch tip. Much attention has been paid on the singular stresses in the theory of elasticity, for example, see Williams [1952], Bogy and Wang [1971], Theocaris [1974], Muskhelishvili [1977], Cherepanov [1979], Atkinson *et al.* [1988], Chen and Nisitani [1993a],

^{††}Corresponding author.

Pageau *et al.* [1994], Sze and Wang [2000], Hills *et al.* [2009], and Lazzarin and Filippi [2006]. In particular, in the case of V-shaped notches, the elastic stress field around the V-shaped notch corner tip behaves like $\sigma \propto 1/r^{1-\lambda}$ with $1/2 < \lambda < 1$, where $\rho\psi$ is measured from the notch tip and λ is the order of stress singularities being intrinsic to the V-shaped notch angle and material property. The order of stress singularities of V-shaped notches is generally weaker than that of cracks.

The singular stress fields of a V-shaped notch depend not only on the intrinsic stress singularities, but also the overall dimension and the external load of a specific structure. The computation of GSIFs related to strength is very important. Above mentioned analytical technique can be applied to some typical problems of simple geometrical discontinuity. However, numerical methods such as integral equation method (IEM) and FEM for the solution of GSIFs have been resorted to in order to deal with complex engineering problems. Chen and Nisitani [1993b, 1995] and Noda and Takase [Noda and Takase (2003); Noda *et al.* (1996)] calculated the GSIFs of the V-shaped single-edged notches in infinite plates and round bars under torsion, tension and bending by using a direct IEM also called the body force method (BFM). Sinclair *et al.* [1984] and Chang and Kang [2002] constructed respectively a set of path independent integrals for the calculation of GSIFs of elastic plates having sharp re-entrant corners or notches with stress-free faces under Mode I, II, or III load. The stress or displacement extrapolation method [Chan *et al.* (1970)] and the hybrid extrapolation method [Kitagawa *et al.* (1984)] can be used directly to solve crack-tip or notch-tip stresses. Barsoum [1976, 1977] used a quarter-point singular element in linear fracture mechanics problems. Liu *et al.* [Liu *et al.* (2011); Nourbakhshnia and Liu (2011)] presented a novel numerical method for effectively simulating the singular stress field for mode-I fracture problems based on the edge-based smoothed finite element method (ES-FEM). The ES-FEM needs only the assumed displacement values on the boundary of the smoothing domains, and hence a new technique to construct singular shape functions is devised for the crack tip elements. Bordas *et al.* [2010], Liu *et al.* [Liu *et al.* (2007); Liu *et al.* (2009)], and Nguyen-Xuan *et al.* [2008] applied strain smoothing for finite elements and proposed suitable extensions to problems with discontinuities and singularities. The numerical results indicate that for 2D and 3D continuum, locking can be avoided. Tur *et al.* [2002] discussed a special finite element to enable the stress state at the apex of a V-shaped notch to be represented in a general model. Munz and Yang [1992] used the traditional finite element technique together with the stress extrapolation method to study singular stress fields at the interface edge of bonded dissimilar materials. Tan and Meguid [1997] derived explicit expressions for the singular stress and displacement fields for a V-shaped notch in bimetals by the use of the Complex Function Method. These expressions were then used to construct a new singular finite element being able to reliably and efficiently determine the singular stress fields and thus the stress intensity factors. Tong and Pian [1973], Lin and Tong [1980], Chen and Sze [2001], and Ping and Chen [Ping *et al.* (2008);

Ping and Chen (2009)] also developed singular notch-tip elements respectively to study the bimaterial notch problems. The list of authors given here is far from being complete due to the large number of researchers having their interest in predicting the fracture behavior of notches.

It is easy to find from aforementioned methods that the FEM is useful for determination of GSIFs of notched configurations. However, it is not yet easy to necessarily obtain the highly accurate values of GSIFs by the conventional FEM. Therefore, in most FEM, the highly accurate numerical solutions of singular stress fields around the notch tips are necessary to resort to in order to obtain satisfactory results, which increase more or less the difficulty of applications of these methods to engineering. Recently, Nisitani [Nisitani *et al.* (1999); Nisitani and Teranishi (2004)] and Noda *et al.* [2006] pointed that the results of SIFs by FE extrapolation analysis may have larger errors, and gave a method for calculating the SIFs with high accuracies in 2D crack or inclusion problems based on the use of the stress values at a crack tip calculated by FEM. However, we are not aware of any researches on V-shaped notch problems with the method have been reported in the literature.

Due to the aforementioned motivation, in this study, the FEM based on the crack tip stress values is extended to deal with the V-shaped notch problems. The method is called as the FEM based on the notch corner tip stresses and does not need special elements accounting for the analytical/or numerical form of singularity. To check the efficiency and versatility of the FEM, the GSIFs of notched strips and notched round bars are numerically solved and compared with reference solutions. As application of present method, GSIFs of step-edged strips and stepped round bars are also discussed.

2. Principle of the Novel Finite Element Method

According to Chen and Nisitani [1993b, 1995]'s study, the GSIFs K_I and K_{II} can be respectively defined as follows:

$$K_I = \lim_{r \rightarrow 0} \sqrt{2\pi r}^{1-\lambda_1} \sigma_{t,r \rightarrow 0}, \quad (1)$$

$$K_{II} = \lim_{r \rightarrow 0} \sqrt{2\pi r}^{1-\lambda_2} \sigma_{nt,r \rightarrow 0}. \quad (2)$$

It has been assumed that $\theta = \beta$ are the angular bisector of the wedge as shown in Fig. 1. λ_1 and λ_2 are orders of stress singularities corresponding to symmetric mode (mode I) and skew-symmetric mode (mode II), respectively, and can be obtained from the eigen-analysis FEM method, for example, see Pageau *et al.* [1994], Sze and Wang [2000], Chen and Sze [2001], Ping *et al.* [2008], and Ping and Chen [2009]. $\sigma_{t,r \rightarrow 0}$ and $\sigma_{nt,r \rightarrow 0}$ stand for respectively the t -direction stress and the shear stress obtained by the FEM near the V-shaped notch corner tip o with respect to the original center of local coordinate system (n, t) .

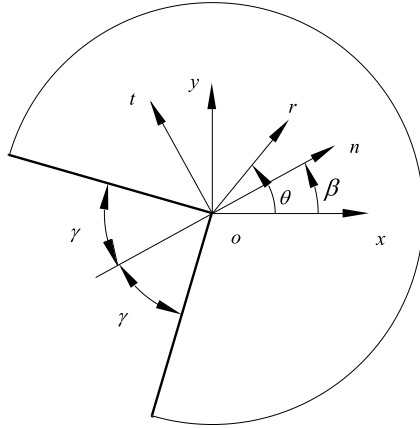


Fig. 1. A V-shaped notch tip domain and the definition of local coordinate system (n, t) .

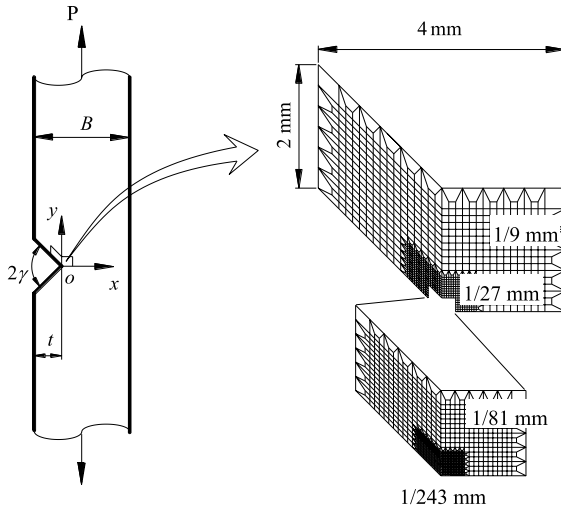


Fig. 2. A single-edged V-shaped notch strip under tension and element pattern around the notch tip.

Figure 2 shows a single-edged V-shaped notch strip under tension and element pattern around the V-shaped notch tip used in the computation. The width of the infinite strip is B , the notch depth is t , and the notch angle $2\gamma = 90^\circ$. In the notch tip domain, the elements are refined systematically, the four-node quadrilateral elements are symmetric with respect to the bisector of notch angle, and the smallest element size e at the V-shaped notch tip is $1/243$ mm, $1/81$ mm, $1/27$ mm or $1/9$ mm.

To explore one-to-one linkage between the V-shaped notch corner tip stress and the GSIF, the curve of the y -direction notch tip stress $\sigma_{y0,FEM}$ obtained by the

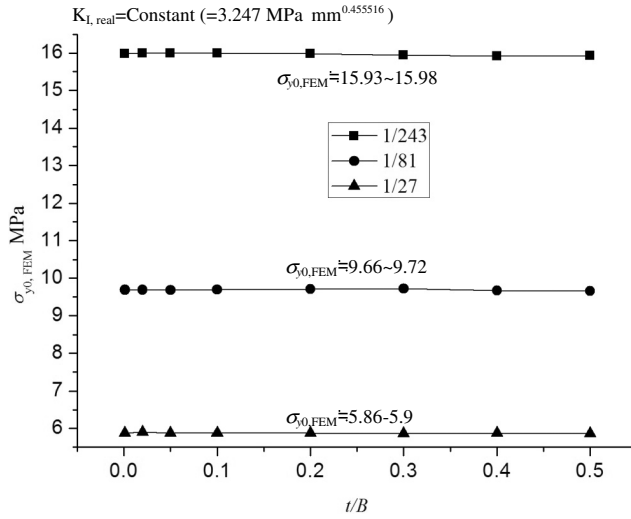


Fig. 3. Relation between $\sigma_{y0,FEM}$ and t/B under the condition of $K_I = \text{constant}$.

FEM vs. dimensionless notch depth t/B under the condition of $K_{I,real} = \text{constant}$ ($= 3.247 \text{ MPa} \cdot \text{mm}^{0.455516}$) is plotted in Fig. 3, where the subscript “real” denotes the exact value of GSIF and “FEM” denote the stresses computed from conventional finite element analysis. The $K_{I,real}$ can be obtained from Chen and Nisitani [1993b], and the value of the y -direction stress $\sigma_{y0,FEM}$ is calculated by the FEM. As seen from Fig. 3, when the value of $K_{I,real}$ keeps unchanged, the stress value at the V-shaped notch corner tip is also nearly constant regardless of the V-shaped notch depth and the smallest element size. This implies that the stress value at a V-shaped notch corner tip from the FEM is very effective as a measurement of the singular stress field at the V-shaped notch corner tip.

Since the ratio of GSIF vs. the V-shaped notch corner tip stress is independent of the V-shaped notch depth, the following equations could be obtained as:

$$\frac{K_{I,real}}{\sigma_{t0,FEM}} = \frac{K_{I,real}^*}{\sigma_{t0,FEM}^*}, \quad \frac{K_{II,real}}{\sigma_{nt0,FEM}} = \frac{K_{II,real}^*}{\sigma_{nt0,FEM}^*}, \quad (3)$$

in which $K_{I,real}$ and $K_{II,real}$ stand for the exact GSIFs of mode I and mode II, respectively, for a given problem and a reference problem; The components with asterisk “*” mean the values of a reference problem.

From Eq. (3), the approximate values of GSIFs $K_{I,appr.}$ and $K_{II,appr.}$ for a given problem can be calculated from the following equations:

$$\frac{K_{I,appr.}}{\sigma_{t,FEM}} = \frac{K_{I,real}^*}{\sigma_{t,FEM}^*}, \quad \frac{K_{II,appr.}}{\sigma_{nt,FEM}} = \frac{K_{II,real}^*}{\sigma_{nt,FEM}^*}. \quad (4)$$

If we use the definition of Eq. (4) of Chen and Nisitani [1993b, 1995], Noda and Takase [2003], and Noda *et al.* [1996], Eq. (4) can be transformed into Eq. (5).

$$F_I = \frac{K_I}{\sigma^\infty \sqrt{\pi} t^{1-\lambda_1}}, \quad F_{II} = \frac{K_{II}}{\sigma^\infty \sqrt{\pi} t^{1-\lambda_2}}, \quad (5)$$

$$F_{I,appr.} = \sigma_{t,FEM} \cdot \frac{F_{I,real}^*}{\sigma_{t,FEM}^*} \cdot \frac{\sigma^{\infty*}}{\sigma^\infty} \cdot \left(\frac{t^*}{t}\right)^{1-\lambda_1}, \quad (6)$$

$$F_{II,appr.} = \sigma_{nt,FEM} \cdot \frac{F_{II,real}^*}{\sigma_{nt,FEM}^*} \cdot \frac{\sigma^{\infty*}}{\sigma^\infty} \cdot \left(\frac{t^*}{t}\right)^{1-\lambda_2},$$

where F_I and F_{II} are dimensionless GSIFs; σ^∞ is a far field stress.

In using Eq. (2), it should be noted that the same mesh pattern and element type around the V-shaped notch corner tip has to be used in the calculation of the notch tip stresses $\sigma_{t,FEM}$, $\sigma_{nt,FEM}$, $\sigma_{t,FEM}^*$ and $\sigma_{nt,FEM}^*$. However, Eq. (2) cannot be yet applied directly to problems having various element sizes at the notch tip because the notch-tip stresses vary with the element sizes. Therefore, when the element size at a notch tip is different from that of a reference problem, the following equation should be used instead of Eq. (2) [Nisitani *et al.* (1999); Nisitani and Teranishi (2004)]:

$$F_{I,appr.} = \sigma_{t,FEM} \cdot \frac{F_{I,real}^*}{\sigma_{t,FEM}^*} \cdot \frac{\sigma^{\infty*}}{\sigma^\infty} \cdot \left(\frac{t^*}{t}\right)^{1-\lambda_1} \cdot \left(\frac{e}{e^*}\right)^{1-\lambda_1}, \quad (7)$$

$$F_{II,appr.} = \sigma_{nt,FEM} \cdot \frac{F_{II,real}^*}{\sigma_{nt,FEM}^*} \cdot \frac{\sigma^{\infty*}}{\sigma^\infty} \cdot \left(\frac{t^*}{t}\right)^{1-\lambda_2} \cdot \left(\frac{e}{e^*}\right)^{1-\lambda_2},$$

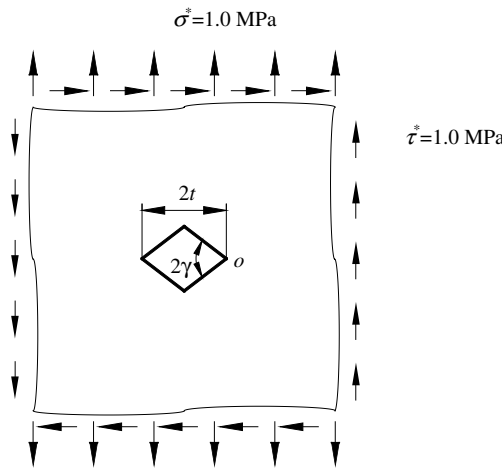


Fig. 4. Configuration of a reference problem.

Table 1. Reference values used for given problems ($\nu = 0.3$).

2γ	Mode I		Mode II	
	$\sigma_{y0,FEM}^*$	$F_{I,real}^*$ [Noda <i>et al.</i> (1996)]	$\sigma_{xy0,FEM}^*$	$F_{II,real}^*$ [Noda <i>et al.</i> (1996)]
30°	30.6114	1.042	11.336	1.154
60°	29.5297	1.148	5.8761	1.599
90°	21.3454	1.336	1.7340	4.279

in which e is the element size at the notch tip. Eq. (7) results from the fact that the stress values near the notch tip decreases or increases proportionally to $1/r^{1-\lambda}$.

In order to obtain $F_{I,appr.}$ and $F_{II,appr.}$ at the vertex of the V-shaped notch corner configuration, the reference values in Eqs. (2) and (7) have to be given firstly. As the reference problem, Fig. 4 shows an infinite plate containing a diamond hole. The fine meshes near the notch tip are divided systematically as shown in Fig. 2, and the element size e^* at the notch tip is set as $1/243$ mm. Table 1 shows the results of notch-tip stresses and the corresponding GSIFs used as the reference values for the given problems in what follows. In order to compare with the reference solutions, the reference values of $F_{I,real}^*$ and $F_{II,real}^*$ in Noda *et al.* [1996] were selected and listed in the table. In the engineering applications, however, the reference values can be calculated approximately with the following equations:

$$F_{I,real}^* = \frac{\lim_{r \rightarrow 0} \sqrt{2\pi} r^{1-\lambda_1} \sigma_{t,r \rightarrow 0}}{\sigma^\infty \sqrt{\pi} t^{1-\lambda_1}}, \tag{8a}$$

$$F_{II,real}^* = \frac{\lim_{r \rightarrow 0} \sqrt{2\pi} r^{1-\lambda_2} \sigma_{nt,r \rightarrow 0}}{\sigma^\infty \sqrt{\pi} t^{1-\lambda_2}}, \tag{8b}$$

where $\sigma_{t,r \rightarrow 0}$ and $\sigma_{nt,r \rightarrow 0}$ are the nodal stresses near singular point o from traditional finite element meshes with refined meshes.

3. Numerical Examples

In the following numerical examples, the Poisson’s ratio is fixed to be 0.3. Mesh pattern in Fig. 2 is used, and the minimum element size e at the V-shaped notch corner tip is $1/243$ mm unless noted otherwise. The far field stresses σ^∞ in Eqs. (4) and (5) are defined as Eqs. (9a)–(9c):

$$\sigma = P/B \quad (\text{for a unit-thickness strip under tension}), \tag{9a}$$

$$\sigma = 6M/B^2 \quad (\text{for a unit-thickness strip under bending}), \tag{9b}$$

$$\sigma = P/\pi B^2 \quad (\text{for a round bar under tension}), \tag{9c}$$

where P and M are far field tension and bending moment, respectively.

In the following Examples 3.1 and 3.2, the V-shaped notch problems of four cases are discussed:

- Case 1: single-edged V-shaped notch problem under tension;
- Case 2: double-edged V-shaped notch problem under tension;
- Case 3: single-edged V-shaped notch problem under bending;
- Case 4: double-edged V-shaped notch problem under bending.

Example 3.1. A single-edged V-shaped notch strip under tension and bending.

As shown in Fig. 5, consider a single-edged V-shaped notch strip under tension and bending. The notch angle and inclined angle are measured by 2γ and β respectively. Herein, 2γ is fixed as 90° . The effects of element size e on accuracy of

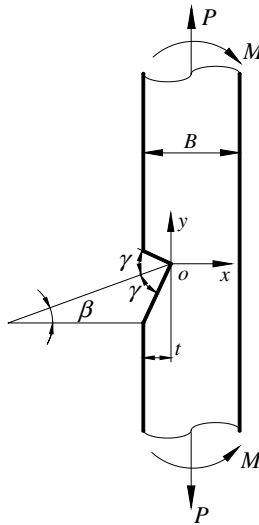


Fig. 5. A single-edged V-shaped notch strip under tension and bending.

Table 2. The effects of element size e on GSIFs $F_{I,appr.}$ of 90° single-edged V-shaped notch strips under tension ($\beta = 0^\circ$).

$\xi = t/B$	$E = 1/243$	$E = 1/81$	$E = 1/27$	$E = 1/9$	Chen and Nisitani [1993b]
0.001	1.336	1.346	1.348	1.346	1.336
0.02	1.340	1.346	1.348	1.346	1.339
0.05	1.359	1.362	1.364	1.362	1.358
0.1	1.419	1.422	1.424	1.422	1.417
0.2	1.630	1.636	1.638	1.635	1.630
0.3	1.975	1.987	1.989	1.982	1.980
0.4	2.514	2.533	2.533	2.516	2.523
0.5	3.381	3.418	3.401	3.358	3.391

GSIFs, $F_{I,appr.}$ and $F_{II,appr.}$, are investigated at first. The GSIFs corresponding to $e = 1/243$ mm, $1/81$, $1/27$ and $1/9$ are listed in Table 2. From Table 2, it can be seen that the maximum relative errors of $\delta F_I (= |F_{I,appr.} - F_{I,BFM}| / \sqrt{F_{I,exact}^2 + F_{II,exact}^2})$ and $\delta F_{II} (= |F_{II,appr.} - F_{II,BFM}| / \sqrt{F_{I,exact}^2 + F_{II,exact}^2})$ are less than about 0.36%, 0.79%, 0.89%, and 0.98% for $e = 1/243$ mm, $1/81$, $1/27$ and $1/9$, respectively. The computational accuracy decreases slightly with increasing element size e . Due to a fact that the present method produces smaller errors of numerical results with

Table 3. The GSIFs $F_{I,appr.}$ and $F_{II,appr.}$ of 90° single-edged V-shaped notch strips under tension.

$\xi = t/B$	$F_{I,appr.}$			$F_{II,appr.}$		
	$\beta = 0^\circ$	$\beta = 15^\circ$	$\beta = 30^\circ$	$\beta = 0^\circ$	$\beta = 15^\circ$	$\beta = 30^\circ$
0.001	1.336(1.336)	1.272(1.266)	1.068(1.065)	0.000(0.000)	0.943(0.946)	1.580(1.576)
0.02	1.340(1.339)	1.275(1.271)	1.072(1.069)	0.000(0.000)	0.945(0.949)	1.586(1.581)
0.05	1.359(1.358)	1.293(1.289)	1.090(1.087)	0.000(0.000)	0.958(0.961)	1.611(1.606)
0.1	1.419(1.417)	1.352(1.347)	1.148(1.146)	0.000(0.000)	0.999(1.001)	1.692(1.687)
0.2	1.630(1.630)	1.562(1.557)	1.358(1.356)	0.000(0.000)	1.136(1.140)	1.980(1.975)
0.3	1.975(1.980)	1.909(1.903)	1.697(1.695)	0.000(0.000)	1.369(1.372)	2.470(2.465)
0.4	2.514(2.523)	2.445(2.441)	2.214(2.211)	0.000(0.000)	1.752(1.760)	3.254(3.254)
0.5	3.381(3.391)	3.304(3.297)	3.030(3.026)	0.000(0.000)	2.426(2.437)	4.559(4.575)
0.6	4.878	4.773	4.423	0.000	3.689	6.967
0.7	7.786	7.637	7.130	0.000	6.408	12.102
0.8	14.928	14.669	13.778	0.000	13.993	26.423
0.9	44.668	43.947	41.832	0.000	52.975	76.237

Note: The values in the parentheses were obtained by Chen and Nisitani [1993b] with the BFM.

Table 4. The GSIFs $F_{I,appr.}$ and $F_{II,appr.}$ of 90° single-edged V-shaped notch strips under bending.

$\xi = t/B$	$F_{I,appr.}$			$F_{II,appr.}$		
	$\beta = 0^\circ$	$\beta = 15^\circ$	$\beta = 30^\circ$	$\beta = 0^\circ$	$\beta = 15^\circ$	$\beta = 30^\circ$
0.001	1.334(1.336)	1.269(1.266)	1.066(1.065)	0.000(0.000)	0.940(0.946)	1.577(1.576)
0.02	1.304(1.303)	1.245(1.237)	1.044(1.042)	0.000(0.000)	0.909(0.909)	1.518(1.514)
0.05	1.267(1.268)	1.207(1.205)	1.021(1.019)	0.000(0.000)	0.859(0.863)	1.445(1.440)
0.1	1.229(1.234)	1.178(1.175)	1.006(1.005)	0.000(0.000)	0.798(0.802)	1.353(1.350)
0.2	1.228(1.233)	1.185(1.182)	1.043(1.043)	0.000(0.000)	0.719(0.721)	1.261(1.260)
0.3	1.297(1.305)	1.263(1.262)	1.149(1.147)	0.000(0.000)	0.692(0.695)	1.286(1.284)
0.4	1.453(1.463)	1.431(1.426)	1.322(1.324)	0.000(0.000)	0.746(0.749)	1.437(1.445)
0.5	1.747(1.750)	1.708(1.715)	1.615(1.611)	0.000(0.000)	0.918(0.930)	1.804(1.816)
0.6	2.265	2.228	2.114	0.000	1.329	2.577
0.7	3.291	3.257	3.075	0.000	2.268	4.297
0.8	5.755	5.708	5.438	0.000	4.842	9.211
0.9	15.867	15.785	14.968	0.000	17.100	34.046

Note: The values in the parentheses were obtained by Chen and Nisitani [1993b] with the BFM.

coarse meshes, it can be used to solve singular problems with fewer elements than the traditional FEM does. The numerical GSIFs at the V-shaped notch corner tip o for $\beta = 0^\circ, 15^\circ$ and 30° , calculated with the refined mesh size $e = 1/243$, are respectively shown in Tables 3 and 4. In these two tables, The $F_{I,BFM}$ and $F_{II,BFM}$

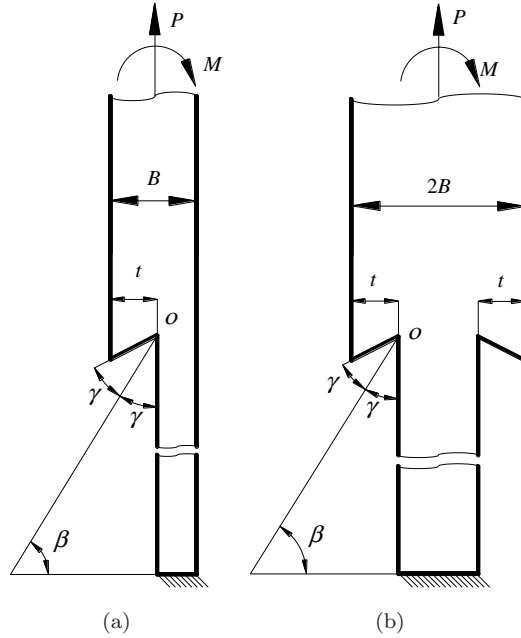


Fig. 6. V-shaped stepped notch strips under tension and bending. (a) A single-edged V-shaped stepped notch strip (b) double-edged V-shaped stepped notch strip.

Table 5. The GSIFs $F_{I,appr.}$ and $F_{II,appr.}$ for 30° V-shaped stepped notch strips.

$\xi = t/B$	$F_{I,appr.}$				$F_{II,appr.}$			
	Case 1	Case 2	Case 3	Case 4	Case 1	Case 2	Case 3	Case 4
0.001	0.370	0.370	0.370	0.370	0.389	0.389	0.389	0.389
0.01	0.376	0.371	0.377	0.373	0.396	0.390	0.393	0.391
0.1	0.455	0.389	0.421	0.416	0.478	0.409	0.406	0.420
0.2	0.575	0.413	0.487	0.476	0.601	0.433	0.434	0.466
0.3	0.746	0.461	0.57	0.555	0.770	0.427	0.477	0.531
0.4	1.005	0.477	0.69	0.664	1.016	0.499	0.547	0.631
0.5	1.424	0.522	0.874	0.828	1.406	0.548	0.669	0.792
0.6	2.141	0.583	1.164	1.093	2.045	0.614	0.870	1.065
0.7	3.547	0.676	1.706	1.582	3.271	0.803	1.270	1.600
0.8	7.009	0.810	3.032	2.727	6.258	0.899	2.313	2.927
0.9	21.298	1.116	7.990	7.224	18.779	1.352	6.444	8.544

Table 6. The GSIFs $F_{I,appr.}$ and $F_{II,appr.}$, for 60° V-shaped stepped notch strips.

$\xi = t/B$	$F_{I,appr.}$				$F_{II,appr.}$			
	Case 1	Case 2	Case 3	Case 4	Case 1	Case 2	Case 3	Case 4
0.001	0.468	0.467	0.466	0.467	0.406	0.406	0.405	0.406
0.01	0.476	0.469	0.473	0.472	0.414	0.408	0.408	0.408
0.1	0.576	0.492	0.522	0.522	0.501	0.427	0.416	0.435
0.2	0.727	0.522	0.592	0.583	0.629	0.452	0.439	0.474
0.3	0.941	0.558	0.684	0.687	0.814	0.482	0.478	0.549
0.4	1.264	0.603	0.822	0.822	1.085	0.52	0.551	0.658
0.5	1.774	0.661	1.028	1.025	1.517	0.57	0.68	0.837
0.6	2.642	0.738	1.361	1.357	2.248	0.642	0.908	1.153
0.7	4.329	0.851	1.988	1.981	3.702	0.754	1.383	1.796
0.8	8.454	1.041	3.464	3.267	7.437	0.961	2.626	3.275
0.9	25.414	1.472	9.220	9.336	24.509	1.508	7.548	11.122

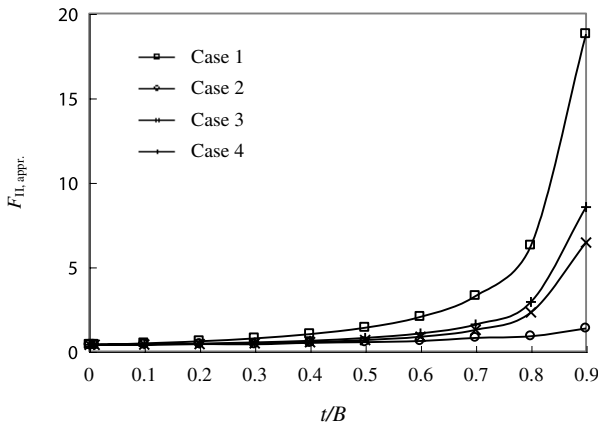
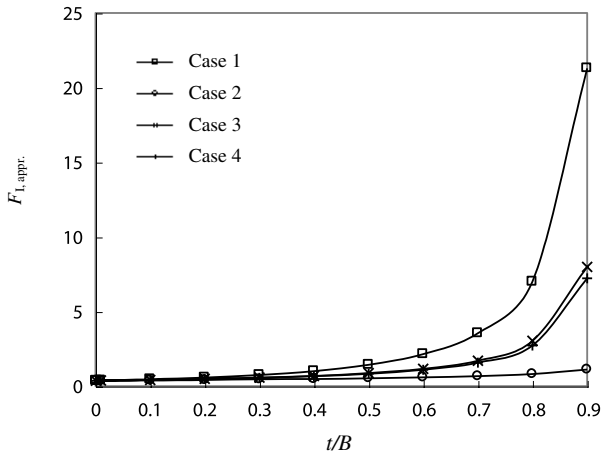


Fig. 7. The GSIFs $F_{I,appr.}$ and $F_{II,appr.}$ of 30° V-shaped stepped notch strips under tension or bending.

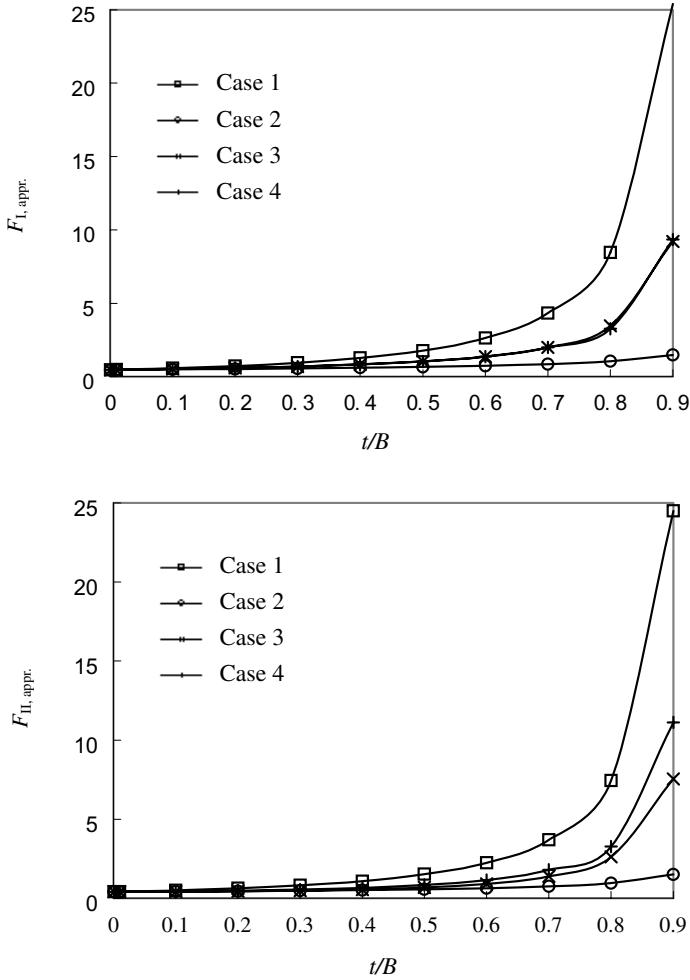


Fig. 8. The GSIFs $F_{I,appr.}$ and $F_{II,appr.}$ of 60° V-shaped stepped notch strips under tension and bending.

resulting from the BFM of Chen and Nisitani [1993b] are also listed in parentheses, and the maximum errors of δF_I and δF_{II} both are less than 0.46%. Therefore, it can be drawn a conclusion that the present method can be used to solve the highly accurate values of GSIFs of the 2D V-shaped notch problems.

Example 3.2. Stepped notch strips under tension or bending.

As applications, two kinds of V-shaped stepped notch infinite strips such as the single-edged V-shaped stepped notch strip and the double-edged V-shaped stepped notch strip shown in Fig. 6 are considered herein. The lower edge of the strip is fixed, and the upper edge of the strip is subjected to tension or bending. The element size

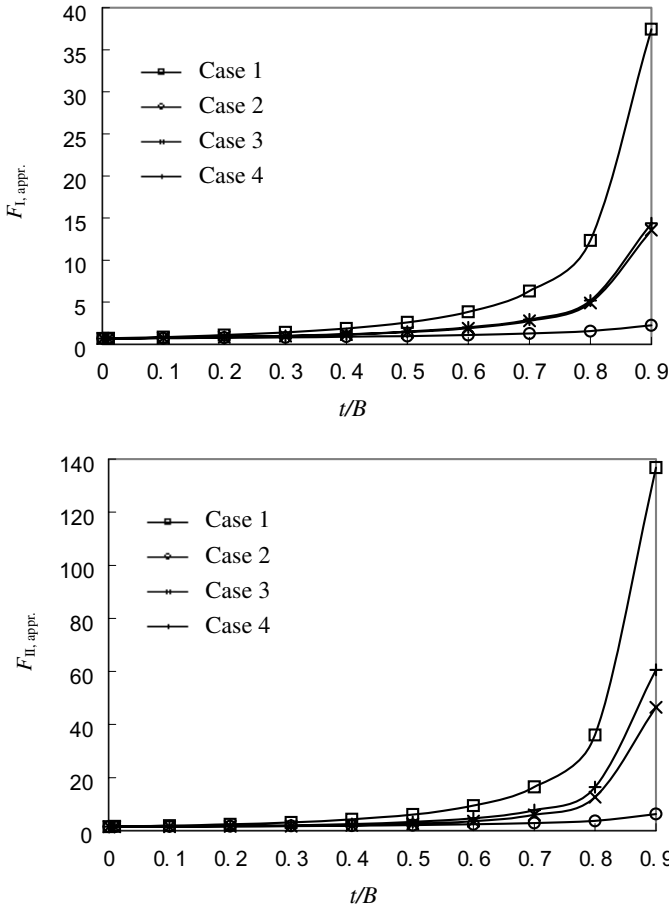


Fig. 9. The GSIFs $F_{I,appr.}$ and $F_{II,appr.}$ of 90° V-shaped stepped notch strips under tension and bending.

$e = 1/243$ is used herein to calculate the GSIFs to obtain more precise solutions. The GSIFs at the V-shaped notch corner tip o vs. t/B corresponding to Cases 1–4 are investigated firstly. The numerical results of GSIFs $F_{I,appr.}$ and $F_{II,appr.}$ for $2\gamma = 30^\circ, 60^\circ$ and 90° are shown in Tables 5–7 and Figs. 7–9, respectively. The results show that the GSIFs increase more and more rapidly with increasing the step height t . On the other hand, it is found that the GSIFs for Case 1 are always the strongest, implying that this case is the most dangerous one and more likely to cause crack initiation comparing with Cases 2–4.

The normalized GSIFs of 90° V-shaped notch problems under Cases 1–4 are respectively shown in Figs. 10–13. It should be noted that among numerical results, the ones for $\beta = 0^\circ, 15^\circ$ and 30° can also be obtained from Chen and Nisitani [1993b] in which the ones for $\beta = 45^\circ$ corresponding to the 90° V-shaped stepped

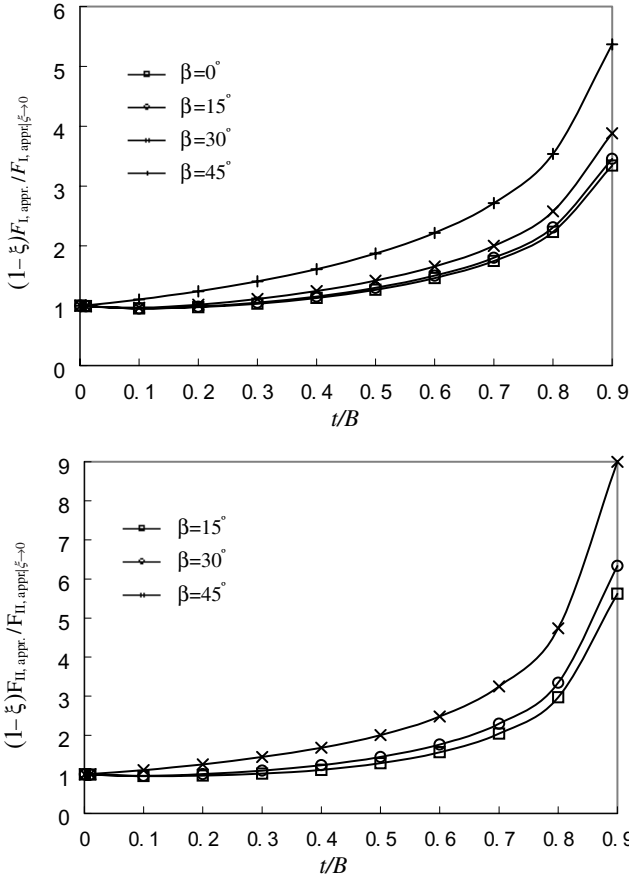


Fig. 10. The normalized GSIFs of single-edged 90° V-shaped notch strips under tension (Case 1).

notch strip are calculated by the present method. The Figs. 10–13 show that the variations of normalized GSIFs for $0^\circ \leq \beta \leq 30^\circ$ are very small, but the ones for $30^\circ \leq \beta \leq 45^\circ$ are much larger. Therefore, for any sizes of V-shaped notch strips with inclined angle $0^\circ < \beta < 30^\circ$, the normalized GSIFs for $\beta = 0^\circ, 15^\circ$ and 30° can be estimated approximately from the present numerical solutions. On the other hand, as the inclined angle is $30^\circ \leq \beta \leq 45^\circ$, it would be better to calculate the normalized GSIFs for each given inclined angle to avoid larger errors.

From the Figs. 10–13, it is easy to find that, if the corner angle and the load are the same, crack initiation in the V-shaped stepped notch strip is easier to happen than it does in the V-shaped notch strip. In addition, it is noticed that the normalized GSIFs $F_{I,appr.}$ and $F_{II,appr.}$ as shown in Fig. 10 increase with the increase of t/B , implying that the singular stresses around the point o are gradually controlled by both extending stresses and shearing stresses with increasing t/B even though the strip is only subjected to far field tension.

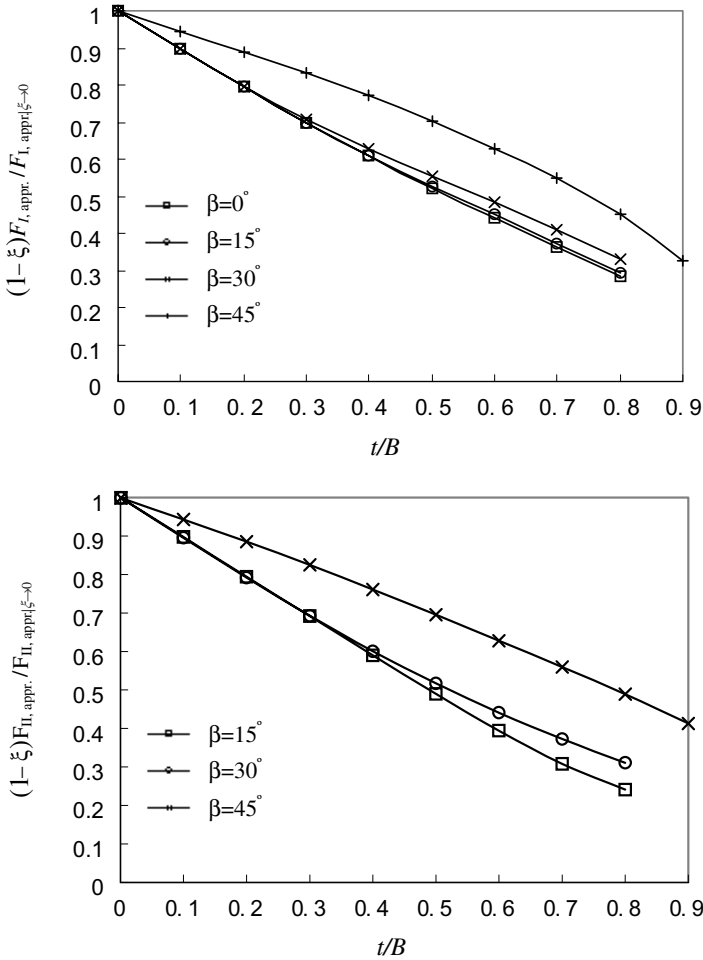


Fig. 11. The normalized GSIFs of double-edged 90° V-shaped notch strips under tension (Case 2).

Example 3.3. Notch round bars under tension.

As shown in Fig. 14 a V-shaped notch round bar and a V-shaped stepped notch round bar under tension are considered. Due to the axis-symmetry of geometry, the models as shown in Fig. 15 are used for the mesh division of the V-shaped notch round bar and the V-shaped stepped notch round bar, respectively. The mesh pattern for the 2D problem is still be used herein, and the 3D mesh can be obtained by rotating the 2D mesh around the central axis of the round bar. The rotation angle θ is set as 0.2° considering that the stress values in the case of $\theta < 1^\circ$ are almost constant [Nisitani and Teranishi (2004)]. The element size $e = 1/243$ is used herein to calculate GSIFs.

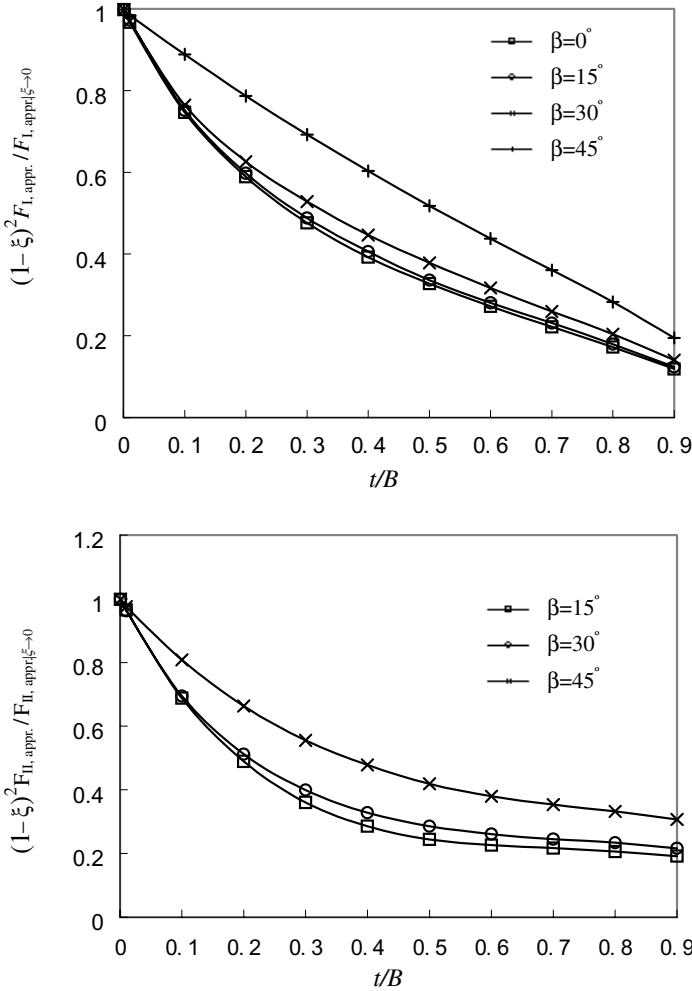


Fig. 12. The normalized GSIFs of single-edged 90° V-shaped notch strips under bending (Case 3).

The V-shaped notch round bar under tension as shown in Fig. 14(a) was considered by Noda and Takase [2003] with the use of the BFM. To check the effectiveness of the present method for solving the V-shaped notch round bar problem, its normalized GSIFs are re-calculated by the present method. The numerical results of normalized GSIFs are listed in Table 8. It can be seen that the present results are in very good agreement with Noda and Takase [2003], and the maximum error of all numerical solutions is less than 1%. Therefore, it is proved that the present method is very effective for the solution of the V-shaped notch round bar problem.

The numerical results of GSIFs for the V-shaped stepped notch round bar under tension vs. t/B is shown in Table 9. It can also be seen that, the GSIFs increase

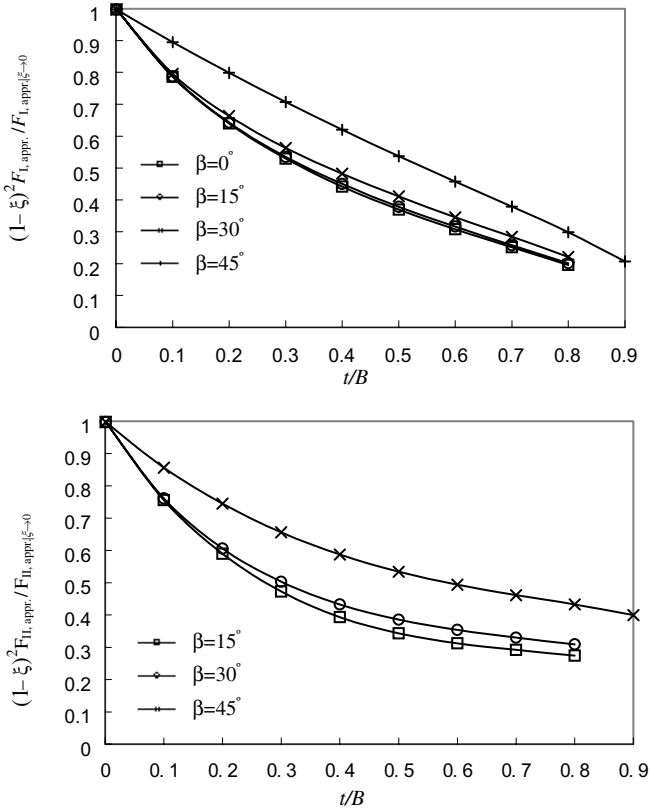


Fig. 13. The normalized GSIFs of double-edged 90° V-shaped notch strips under bending (Case 4).

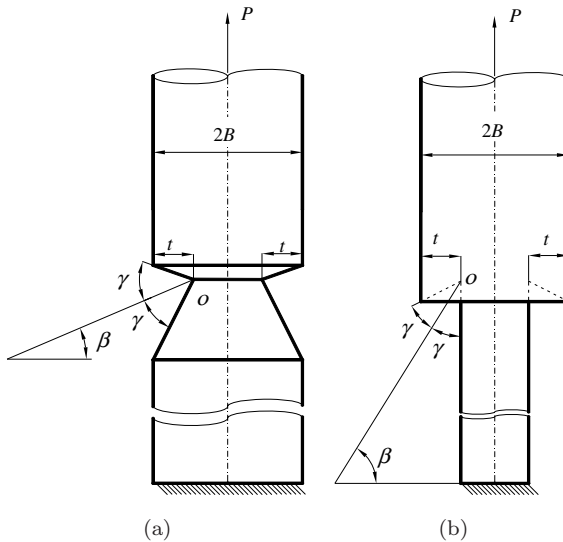


Fig. 14. V-shaped notch round bars. (a) A V-shaped notch round bar. (b) A V-shaped stepped round bar.

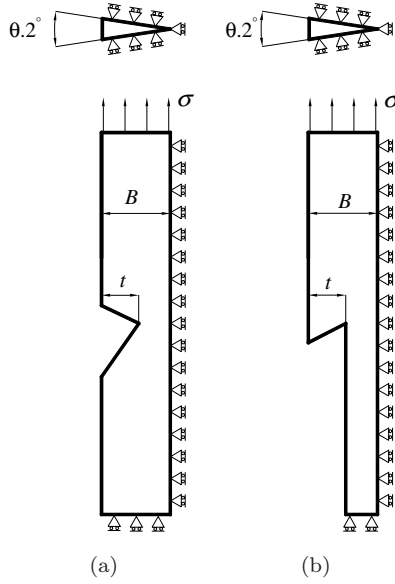


Fig. 15. The models used for mesh division. (a) The notched round bar. (b) The stepped round bar.

Table 7. The GSIFs $F_{I,appr.}$ and $F_{II,appr.}$ for 90° V-shaped stepped notch strips.

$\xi = t/B$	$F_{I,appr.}$				$F_{II,appr.}$			
	Case 1	Case 2	Case 3	Case 4	Case 1	Case 2	Case 3	Case 4
0.001	0.697	0.697	0.696	0.696	1.520	1.519	1.515	1.517
0.01	0.708	0.698	0.699	0.701	1.543	1.520	1.507	1.519
0.1	0.856	0.732	0.763	0.769	1.874	1.592	1.511	1.604
0.2	1.081	0.776	0.855	0.869	2.386	1.682	1.569	1.765
0.3	1.400	0.829	0.983	1.005	3.128	1.790	1.716	2.032
0.4	1.872	0.895	1.165	1.200	4.254	1.927	2.011	2.476
0.5	2.609	0.981	1.442	1.497	6.092	2.112	2.538	3.242
0.6	3.867	1.098	1.904	1.992	9.417	2.385	3.597	4.681
0.7	6.315	1.272	2.789	2.934	16.456	2.833	5.948	7.778
0.8	12.331	1.570	4.918	5.196	36.028	3.713	12.576	16.419
0.9	37.441	2.263	13.576	14.392	136.777	6.268	46.521	60.638

with increasing t/B . It should be noted that it is meaningless to compare the GSIFs among $\gamma = 15^\circ, 30^\circ$ and 45° , because the intrinsic stress singularities of them are different. The normalized values of $(1 - \xi)^2 F_{I,appr.}/F_{I,appr.|\xi \rightarrow 0}$ and $(1 - \xi)^2 F_{II,appr.}/F_{II,appr.|\xi \rightarrow 0}$ are also listed in Table 9. It is obvious that the absolute values of the normalized GSIFs for the V-shaped stepped notched round bars are larger than those for the V-shaped notch round bars with the same γ and t/B .

Table 8. The normalized GSIFs of 90° V-shaped notch round bars under tension.

$\xi = t/B$	$F_{I,appr. \xi \rightarrow 0} / (1 - \xi)^2 F_{I,appr.} /$			$F_{I,exact \xi \rightarrow 0} / (1 - \xi)^2 F_{I,exact} /$			$F_{II,appr. \xi \rightarrow 0} / (1 - \xi)^2 F_{II,appr.} /$			$F_{II,exact \xi \rightarrow 0} / (1 - \xi)^2 F_{II,exact} /$		
	[Noda and Takase (2003)]			[Noda and Takase (2003)]			[Noda and Takase (2003)]			[Noda and Takase (2003)]		
	$\beta = 0^\circ$	$\beta = 15^\circ$	$\beta = 30^\circ$	$\beta = 0^\circ$	$\beta = 15^\circ$	$\beta = 30^\circ$	$\beta = 0^\circ$	$\beta = 15^\circ$	$\beta = 30^\circ$	$\beta = 0^\circ$	$\beta = 15^\circ$	$\beta = 30^\circ$
0.001	0.998	0.998	0.998	0.998	0.998	0.998	0.000	0.998	0.998	0.000	0.998	0.998
0.01	0.985	0.985	0.991	0.985	0.985	0.983	0.000	0.983	0.997	0.000	0.984	0.982
0.1	0.851	0.850	0.859	0.852	0.854	0.856	0.000	0.839	0.849	0.000	0.843	0.840
0.5	0.435	0.443	0.485	0.434	0.446	0.485	0.000	0.382	0.436	0.000	0.385	0.434
0.9	0.160	0.166	0.189	0.161	0.168	0.189	0.000	0.223	0.281	0.000	0.229	0.282

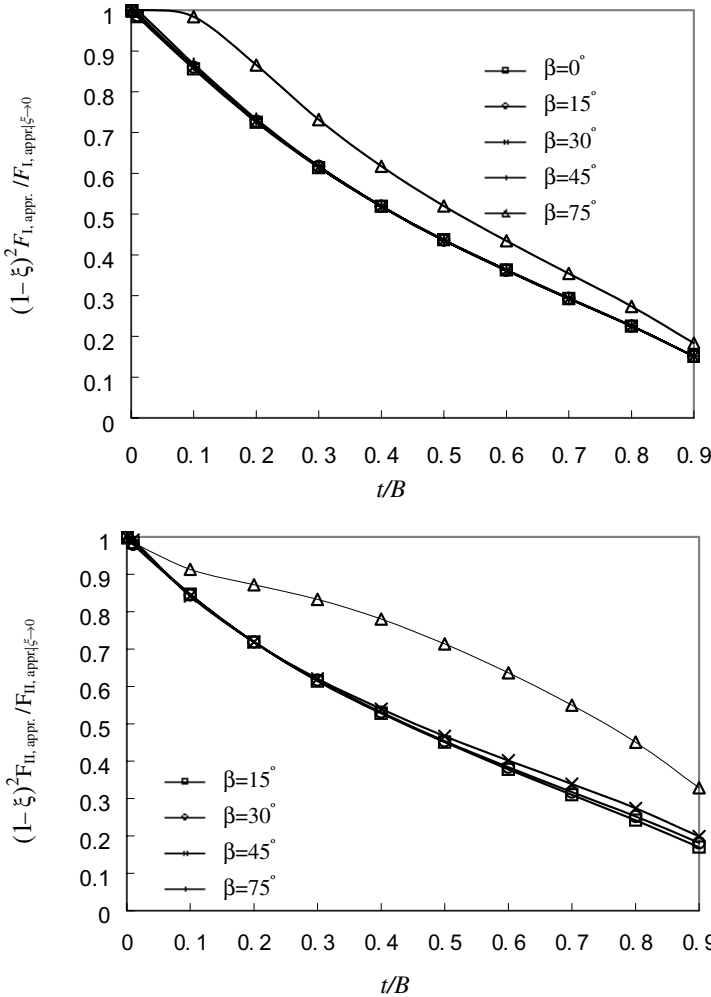


Fig. 16. The normalized GSIFs of V-shaped notch round bars under tension when $\gamma = 15^\circ$.

For different β corresponding to half notch angle $\gamma = 15^\circ$ and 30° , the normalized GSIFs for the V-shaped notch round bars vs. t/B for are plotted in Figs. 16 and 17, respectively, and those for different β corresponding to $\gamma = 45^\circ$ are then depicted in Fig. 18. In Figs. 16–18, the results for the V-shaped notch round bars can also be obtained from Chen and Nisitani [1995] in which the results for stepped notched round bars are not given. From the Figs. 16–18, the same conclusion can be drawn as mentioned above that, if t/B is the same, the variations of the normalized GSIFs of the V-shaped notch round bars are small and almost independent of β for $0^\circ \leq \beta \leq 30^\circ$. This implies that, for any V-shaped notch round bars with the inclined angle $0^\circ \leq \beta \leq 30^\circ$, their normalized GSIFs can be estimated approximately from

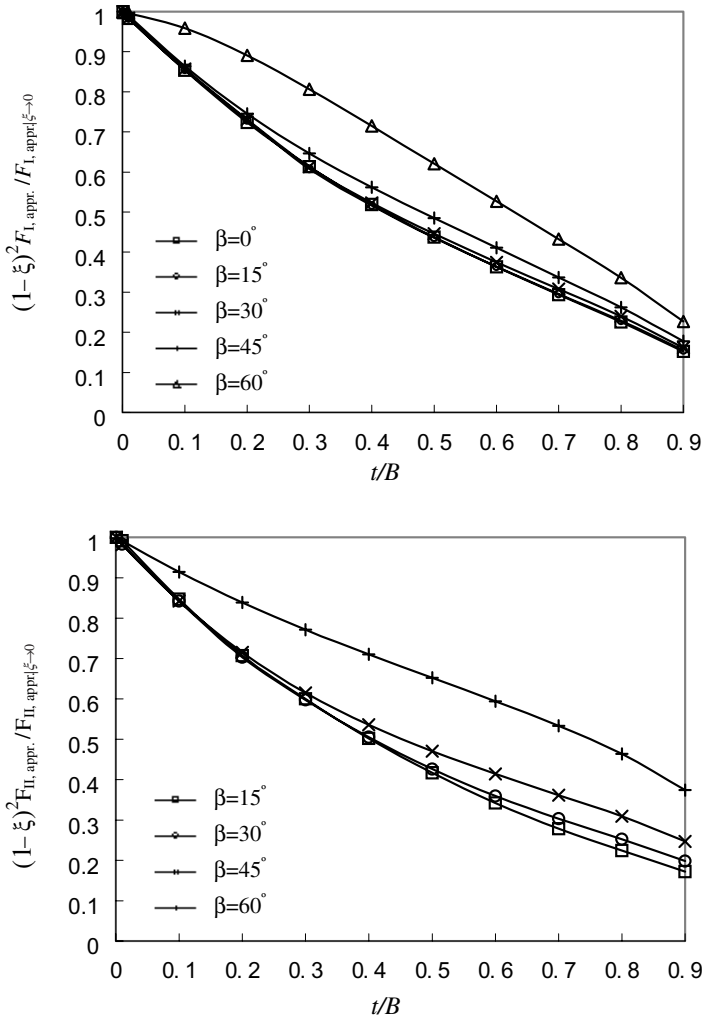


Fig. 17. The normalized GSIFs of V-shaped notch round bars under tension when $\gamma = 30^\circ$.

the present results. However, when the V-shaped notch round bars become the V-shaped stepped notch round bars (corresponding to the curves for $\beta = 75^\circ$ and $\gamma = 15^\circ$ in Fig. 16, $\beta = 60^\circ$ and $\gamma = 30^\circ$ in Fig. 17 and $\beta = 45^\circ$ and $\gamma = 45^\circ$ in Fig. 18), the aforementioned conclusion is untenable because the variations of the normalized values of GSIFs for the V-shaped stepped notched round bars are larger than those for the V-shaped notch round bars. It implies that the conclusion is not suitable for the V-shaped stepped notch round bar although it is one special form of the V-shaped notch round bars.

Likewise, according to the Figs. 16–18, it can be seen that, if the V-shaped notch corner angle and the far field load are the same, crack initiation in the V-shaped

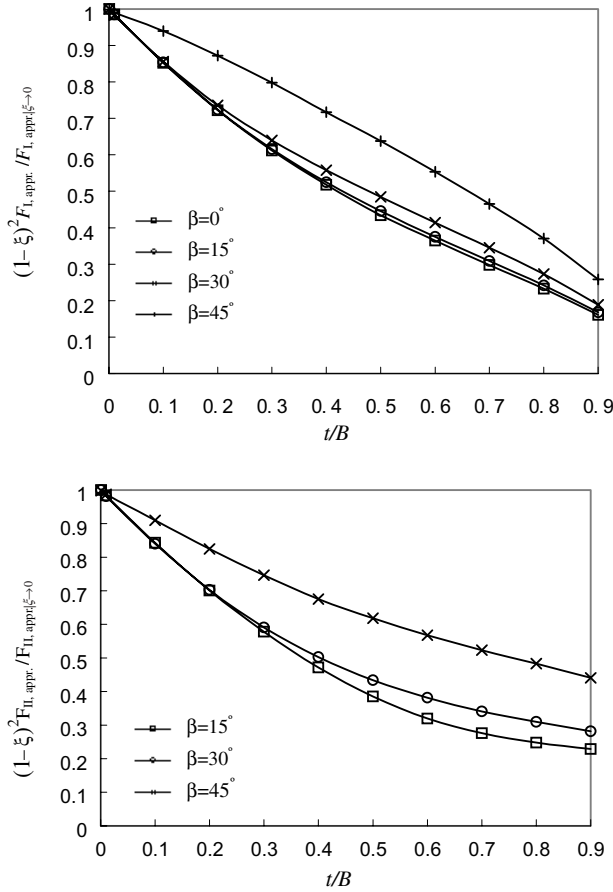


Fig. 18. The normalized GSIFs of V-shaped notch round bars under tension when $\gamma = 45^\circ$.

Table 9. The GSIFs $F_{I,appr.}$ and $F_{II,appr.}$ for V-shaped stepped notch round bars.

$\xi = t/B$	$F_{I,appr.} \cdot ((1 - \xi)^2 F_{I,appr.} / F_{I,appr. \xi \rightarrow 0})$			$F_{II,appr.} \cdot ((1 - \xi)^2 F_{II,appr.} / F_{II,appr. \xi \rightarrow 0})$		
	$\gamma = 15^\circ$	$\gamma = 30^\circ$	$\gamma = 45^\circ$	$\gamma = 15^\circ$	$\gamma = 30^\circ$	$\gamma = 45^\circ$
0.001	0.371(0.998)	0.515(0.998)	0.698(0.998)	0.389(0.998)	0.563(0.998)	1.519(0.998)
0.01	0.379(1.001)	0.523(0.995)	0.705(0.990)	0.391(0.985)	0.569(0.991)	1.531(0.988)
0.1	0.451(0.985)	0.610(0.959)	0.809(0.939)	0.439(0.914)	0.635(0.914)	1.706(0.910)
0.2	0.502(0.866)	0.717(0.891)	0.951(0.872)	0.531(0.874)	0.737(0.838)	1.958(0.825)
0.3	0.554(0.732)	0.848(0.806)	1.136(0.797)	0.662(0.834)	0.886(0.771)	2.313(0.746)
0.4	0.636(0.617)	1.022(0.714)	1.390(0.717)	0.844(0.781)	1.110(0.710)	2.850(0.675)
0.5	0.772(0.520)	1.279(0.621)	1.779(0.637)	1.112(0.715)	1.468(0.652)	3.756(0.618)
0.6	1.007(0.434)	1.696(0.527)	2.412(0.553)	1.550(0.638)	2.089(0.594)	5.386(0.567)
0.7	1.459(0.354)	2.477(0.432)	3.606(0.465)	2.380(0.551)	3.332(0.533)	8.831(0.523)
0.8	2.536(0.273)	4.329(0.336)	6.458(0.370)	4.392(0.452)	6.522(0.463)	18.36(0.483)
0.9	6.808(0.184)	11.702(0.227)	18.012(0.258)	12.800(0.329)	21.031(0.374)	66.949(0.441)

stepped notch round bars is easier to happen than it does in the V-shaped notch round bars.

Conclusions

A novel FE analysis technique has been developed to solve the GSIFs around a V-shaped notch corner tip. The method does not need special elements accounting for the analytical or numerical form of singularities; therefore, it is very applicable and suitable for engineers to solve such engineering problems. As its applications, the V-shaped notch strips, V-shaped stepped notch strips, V-shaped notch round bars and V-shaped stepped notch round bars under tension or bending are discussed with the present method. Some useful conclusions in the following can be drawn as:

- (1) The present method can be used to obtain highly accurate values of GSIFs of any V-shaped notch problems with coarse meshes without accounting for the analytical/or numerical form of singular stress fields.
- (2) The normalized GSIFs of any V-shaped notch problems for $0^\circ \leq \beta \leq 30^\circ$ can be estimated approximately from the present numerical results, but those of any V-shaped stepped notch problems do not hold water.
- (3) If the V-shaped notch corner angle and the far field load are the same, crack initiation with respect to the V-shaped stepped notch problems is easier to happen than it does with respect to the V-shaped notch problems.
- (4) The singular stresses around the point o are gradually controlled by both extending stresses and shearing stresses with increasing the notch depth t/B even though the strip or round bar is only subjected to far field tension.

Acknowledgments

The authors are grateful for the suggestions and comments of the reviewers. This study was supported by Kyushu Institute of Technology Fellowship for Foreign Researchers, and part of this study was sponsored by the National Natural Science Foundation of China through Grant Nos. 51065008, 10362002 and 10662004, the Natural Science Foundation of Jiangxi Province through Grant Nos. 2010GZW0013 and 2007GZW0862 and the Jinggang-Star Training Plan for Young Scientists of Jiangxi Province through Grant No. 20112BCB23013.

References

- Atkinson, C., Bastero, J. M. and Martínez-Esnaola, J. M. [1988] "Stress analysis in sharp angular notches using auxiliary fields," *Eng. Fract. Mech.* **31**, 637–646.
- Barsoum, R. S. [1976] "On the use of isoparametric finite elements in linear fracture mechanics," *Int. J. Numer. Methods Eng.* **10**(1), 25–37.
- Barsoum, R. S. [1977] "Triangular quarter-point elements as elastic and perfectly-plastic crack tip elements," *Int. J. Numer. Methods Eng.* **11**(1), 85–98.
- Bogy, D. B. and Wang, K. C. [1971] "Stress singularities at interface corners in bonded dissimilar isotropic elastic materials," *Int. J. Solids Struct.* **7**, 993–1005.

- Bordas, S., Rabczuk, T., Nguyen-Xuan, H., Nguyen Vinh, P., Natarajan, S., Bog, T., Do Minh, Q. and Nguyen Vinh, H. [2010] "Strain smoothing in FEM and XFEM," *Comput. Struct.* **88**(23–24), 1419–1443.
- Chan, S. K., Tuba, I. S. and Wilson, W. K. [1970] "On the finite element method in linear elastic fracture mechanics," *Eng. Fract. Mech.* **2**(1), 1–17.
- Chang, J. H. and Kang, L. K. [2002] "Evaluation of the stress field around a notch tip using contour integrals," *Int. J. Eng. Sci.* **40**(5), 569–586.
- Chen, D. H. and Nisitani, H. [1993a] "Singular stress fields near a corner of jointed dissimilar materials," *ASME J. Appl. Mech.* **60**(3), 607–613.
- Chen, D. H. and Nisitani, H. [1993b] "Stress intensity factors K_{I,λ_1} and K_{II,λ_2} of a strip with a V-shaped single notch under tension or in-plane bending," *Trans. JSME (A)* **59**–560, 1069–1073 (in Japanese).
- Chen, D. H. and Nisitani, H. [1995] "Stress intensity factors for V-notched strip under tension on in-plane bending," *Int. J. Fract.* **70**(1), 81–97.
- Chen, M. C. and Sze, K. Y. [2001] "A novel hybrid finite element analysis of bimaterial notch problems," *Eng. Fract. Mech.* **68**(13), 1463–1476.
- Cherepanov, G. P. [1979] *Mechanics of Brittle Fracture* (McGraw-Hill, New-York).
- Hills, D. A., Dini, D., Magadu, A. and Korsunsky, A. M. [2009] "A review of asymptotic procedures in stress analysis: Known solutions and their applications," *The J. Strain Anal. Eng. Des.* **39**(2), 553–568.
- Kitagawa, H., Yuuki, R., Kisu, H. and Kawabata, H. [1984] "The analysis of stress intensity factor of surface crack by boundary element method," *Trans. JSME (A)* **50**–450, 129–138 (in Japanese).
- Lazzarin, P. and Filippi, S. [2006] "A generalised stress intensity factor to be applied to rounded V-shaped notches," *Int. J. Solids Struct.* **43**(9), 2461–2478.
- Lin, K. Y. and Tong, P. [1980] "Singular finite elements for the fracture analysis of V-notched plate," *Int. J. Numer. Methods Eng.* **15**(9), 1343–1354.
- Liu, G. R., Dai, K. Y. and Nguyen-Thoi, T. [2007] "A smoothed finite element for mechanics problems," *Comput. Mech.* **39**(6), 859–877.
- Liu, G. R., Nguyen-Thoi, T., Nguyen-Xuan, H. and Lam, K. Y. [2009] "A node based smoothed finite element method (NS-FEM) for upper bound solution to solid mechanics problems," *Comput. Struct.* **87**(1–2), 14–26.
- Liu, G. R., Nourbakhshia, N. and Zhang, Y. W. [2011] "A novel singular ES-FEM method for simulating singular stress fields near the crack tips for linear fracture problems," *Eng. Fract. Mech.* **78**(6), 863–876.
- Munz, D. and Yang, Y. Y. [1992] "Stress singularities at the interface in bonded dissimilar materials under mechanical and thermal loading," *ASME J. Appl. Mech.* **59**(4), 857–861.
- Muskhelishvili, N. I. [1977] *Some Basic Problems of the Mathematical Theory of Elasticity* (Noordhoff Int. Pub., Leyden, The Netherlands).
- Nguyen-Xuan, H., Rabczuk, T., Bordas, S. and Debongnie, J. F. [2008] "A smoothed finite element method for plate analysis," *Comput. Methods Appl. Mech. Eng.* **197**(13–16), 1184–1203.
- Nisitani, H., Kawamura, T., Fujisaki, W. and Fukuda, T. [1999] "Determination of highly accurate values of stress intensity factor or stress concentration factor of plate specimen by FEM," *Trans. JSME (A)* 65–629, 26–31 (in Japanese).
- Nisitani, H. and Teranishi, T. [2004] " K_I of a circumferential crack emanating from an ellipsoidal cavity obtained by the crack tip stress method in FEM," *Eng. Fract. Mech.* **71**(4–6), 579–585.

- Noda, N. A., Chen, K. R., Tajima, K., Imoto, H. and Tsutsumi, T. [2006] "Intensity of singular stress field due to wedge-shaped defect in human tooth after restored with composite resins," *J. Soc. Mater. Sci. Japan* **55**(12), 1060–1066.
- Noda, N. A., Oda, K. and Inoue, T. [1996] "Analysis of newly-defined stress intensity factors for angular corners using singular integral equations of body force method," *Int. J. Fract.* **76**(3), 243–261.
- Noda, N. A. and Takase, Y. [2003] "Generalized stress intensity factors of V-shaped notch in a round bar under torsion, tension and bending," *Eng. Fract. Mech.* **70**(11), 1447–1466.
- Nourbakhshnia, N. and Liu, G. R. [2011] "A quasi-static crack growth simulation based on the singular ES-FEM," *Int. J. Numer. Methods Eng.* **88**(5), 473–492.
- Pageau, S. S., Joseph, P. F. and Biggers, S. B. [1994] "The order of stress singularities for bonded and disbonded three-material junctions," *Int. J. Solids Struct.* **31**(21), 2979–2997.
- Ping, X. C., Chen, M. C. and Xie, J. L. [2008] "Singular stress analyses of V-notched anisotropic plates based on a novel finite element method," *Eng. Fract. Mech.* **75**(13), 3819–3838.
- Ping, X. C. and Chen, M. C. [2009] "Effective elastic properties of solids with irregularly shaped inclusions," *Int. J. Mech. Mater. Des.* **5**(3), 231–242.
- Sinclair, G. B., Okajima, M. and Griffin, J. H. [1984] "Path independent integrals for computing stress intensity factors at sharp notches in elastic plates," *Int. J. Numer. Meth. Eng.* **20**(6), 999–1008.
- Sze, K. Y. and Wang, H. T. [2000] "A simple finite element formulation for computing stress singularities at bimaterial interfaces," *Finite Elem. Anal. Des.* **35**(2), 97–118.
- Tan, M. A. and Meguid, S. A. [1997] "Analysis of bimaterial wedges using a new singular finite element," *Int. J. Fract.* **88**(4), 373–391.
- Theocaris, P. S. [1974] "The order of singularity at a multi-wedge corner of a composite plate," *Int. J. Eng. Sci.* **12**(2), 107–120.
- Tong, P. and Pian, T. H. H. [1973] "On the convergence of the FEM for problems with singularity," *Int. J. Solids Struct.* **9**(3), 313–321.
- Tur, M., Fuenmayor, J., Mugadu, A. and Hill, D. A. [2002] "On the analysis of singular stress fields Part I: Finite element formulation and application to notches," *The J. Strain Anal. Eng. Des.* **37**(5), 437–444.
- Williams, M. L. [1952] "Stress singularities resulting from various boundary conditions in angular corners of plates in extension," *J. Appl. Mech.* **19**(4), 526–528.